LA-UR-92-203

LA-UR--92-203

DE92 007435

Los Alamos National Laboratory is operated by the University of California for the United States Department of Energy under contract W-7405-ENG-36

TITLE: TRAC-PF1/MOD2 BEST-ESTIMATE ANALYSIS OF A LARGE-BREAK LOCA IN A 15 X 15 GENERIC FOUR-LOOP WESTINGHOUSE NUCLEAR POWER PLANT

AUTHOR(S): J. W. Spore
J. C. Lin
N. M. Schnurr
J. R. White
M. C. Cappiello

SUBMITTED TO: The 28th ASME/AIChe/ANS National Heat Transfer Conference
August 9-12, 1992
San Diego, California

DISCLAIMER

Los Alamos
Los Alamos National Laboratory
Los Alamos, New Mexico 87545

TRAC-PF1/MOD2 BEST-ESTIMATE ANALYSIS OF A LARGE-BREAK LOCA IN A 15 X 15 GENERIC FOUR-LOOP WESTINGHOUSE NUCLEAR POWER PLANT

by
Jay W. Spore, J. C. Lin, N. M. Schnurr, J. R. White, and M. C. Cappiello

Engineering and Safety Analysis Group
Nuclear Technology and Engineering Division
Los Alamos National Laboratory
Los Alamos, New Mexico

ABSTRACT

Calculations of a large-break loss-of-coolant accident (LOCA) in a 15 x 15 generic four-loop Westinghouse nuclear power plant with both the TRAC-PF1/MOD1 and TRAC-PF1/MOD2 computer codes[1,2] will be presented. The Transient Reactor Analysis Code (TRAC) has been developed by Los Alamos National Laboratory to provide advanced best-estimate simulations of real postulated transients in pressurized light-water reactors (LWRs) and for many related thermal-hydraulic facilities.

The latest released version of TRAC is TRAC-PF1/MOD2. Significant improvements and enhancements over the MOD1 version were implemented in the MOD2 heat-transfer and constitutive models. One of the most significant improvements in the MOD2 code has been the implementation of the two-step[3,4] numerics method in the three-dimensional components, which can significantly reduce run times for long, slow transients. A very important area of improvement has been in the reflood heat-transfer models.

Developmental assessment results (i.e., code comparisons with experimental data) will be discussed for several separate-effects and integral tests, including analysis of the Upper Plenum Test Facility[5] (UPTF), the Cylindrical Core Test Facility[6] (CCTF), and the Loss-of-Fluid Test Facility[7] (LOFT). The assessment results provide information on the anticipated accuracy for the best-estimate models in the MOD2 computer code. The MOD1 to MOD2 comparison will provide an estimate for the effect of improved heat-transfer models on predicted peak cladding temperatures.

INTRODUCTION

Version 14.4 of the TRAC-PF1/MOD1 code was released as the final version of MOD1 in July 1988. A limited release of the TRAC-PF1/MOD2 code occurred in November of 1990 (Version 5.3). The MOD2 code used the MOD1 code and corrected a number of errors in it and added a number of new features and enhancements. The principal features of the MOD2 code are as follows.

1. A variable-dimensional fluid dynamics model that can address three-dimensional (3D) flow in the vessel component while the loop components (both primary and secondary) are treated as one-dimensional (1D) flow components. It should be noted that a user can specify a 1D vessel component, which will result in reduced computer costs.

2. Two-step numerics in both the 1D and the 3D hydrodynamic components. The two-step numerics allow TRAC to take large time steps during a relatively slow transient, for example, a small break or operational transient. The MOD1 3D vessel numerics will tend to hold the time-step size back during relatively slow transients.

3. A nonhomogeneous, nonequilibrium, full two-fluid, six equation, hydrodynamics model that describes the steam-water flow. A horizontal stratified flow model has been added to the one-dimensional hydrodynamics. A seventh field equation (mass balance) that describes a noncondensable gas field and an eighth field equation that tracks the solutes in the liquid phase also have been added to the TRAC hydrodynamics model.

4. A component-specific, flow-regime-dependent constitutive equation package that describes the transfer of mass, energy, and momentum between the steam-water phases and the interaction of these phases with the heat flow from the system structures.

5. Flow-regime-dependent wall-to-fluid heat-transfer correlations that are obtained from a generalized boiling curve based on local conditions.

6. A two-dimensional (2D) fuel rod conduction model that includes a dynamic fine-mesh rezoning capability that can resolve both bottom flood and falling film quench fronts.

7. A consistent analysis of entire accident sequences, including the initial conditions and the blowdown, refill, and reflood phases of a LOCA. In addition, TRAC can be used to simulate a complete spectrum of break sizes as well as operational transients.

8. Component and functional modularity, which allows the user to model virtually any pressurized water reactor (PWR) design or experimental configuration. TRAC has component models for accumulators, breaks, fills, cores, pipes, pressurizers, pumps, steam generators, turbines, valves, and vessels with associated internals.

9. Trip and control models that give the user the flexibility to model virtually any PWR control or protection system or any experimental control system.

10. Multiple-component connections to a single cell in a vessel component that allow for coarse 3D noding and reduced computer costs.

11. A self-initialization capability that will drive the TRAC model from steady state to a user-specified set of conditions.

12. A counter-current flow-limiting (CCFL)[8] model that allows the user to select from one of several available correlations.

13. A mechanistic steam separator model based on the TRAC-BWR code.

14. Inversion of the vessel data base results in coding for the vessel component that is easier to read and maintain. In addition, it results in arrays that can be vectorized on Cray or Cray-like operating systems.

15. A generalized heat structure component that allows the user to connect any hydro cell in their TRAC model with any other hydro cell. This component results in increased accuracy for the modeling of steam generators, vessel internal structures, etc. In addition, this component gives the TRAC user more flexibility.

16. A new reflood model based on Ishii's flow-regime map.[9]

17. A conserving-momentum flux solution in the MOD2 code.

18. An improvement to the MOD1 wall-shear model in the MOD2 code with fixes to the laminar flow model, inclusion of the surface roughness effect in the turbulent regime, and improvements to the two-phase pressure drop model.

19. A MOD2 valve model based on experimental data for partially closed globe valves.

20. Correction of a problem with the Gauss-Seidel numerical solution for the 3D vessel pressure matrix equation, which was observed to be inaccurate for small breaks and operational transients. This inaccuracy typically would be observed as a mass error in the vessel component. This problem was solved in the MOD2 code by eliminating the Gauss-Seidel method and developing and implementing a capacitance method for solving the vessel pressure matrix equations.

21. A subcooled boiling model in the MOD2 code based on the TRAC-BWR subcooled boiling model.[10]

22. Addition of a general orientation and magnitude of the vessel component for the gravitational acceleration vector option to the MOD2 code. This option was developed to address the horizontal tube modeling problems encountered during the recent applications of the MOD2 code.

23. Addition of 60-, 120-, and 180- degree rotational symmetries in the cylindrical geometry option to the MOD2 code. This option was developed to allow for flexible vessel noding and allows for significantly reduced noding if loop and vessel behaviors are symmetric.

24. Implementation of the United Kingdom Atomic Energy Agency (UKAEA) offtake model[11] for calculation of small breaks in the side, bottom, or top of a large pipe.

25. Implementation of the Japan Atomic Energy Research Institute (JAERI) fully implicit 2D conduction model[12] to reduce computer costs for reflood calculations that required small axial noding.

26. Addition of a critical flow model for subcooled and two-phase choking conditions.

27. Implementation of the ANS 1979 Decay Heat Standard.[13]

28. Addition of the UKAEA standoff thermocouple model.[14]

ASSESSMENT RESULTS

Upper Plenum Test Facility Cold-Leg Flow Test

Description of UPTF. The UPTF is a full-scale model of a four-loop, 1300-MWe PWR and includes the reactor vessel, downcomer, lower plenum, core simulation, upper plenum, and four loops with pump and steam-generator simulation. A flow diagram of the system and an artist's view of the test facility are shown in Fig. 1. The thermal-hydraulic feedback of the containment is simulated with a containment simulator. The test vessel, core barrel, and internals compose a full-size simulation of a PWR with four full-scale hot and cold legs simulating three intact loops and one broken loop.

Both cold- and hot-leg breaks can be investigated in the UPTF, including emergency core-coolant (ECC) injection into the intact and broken cold and/or hot legs and into the downcomer. The steam produced in a real core and the water entrained by this steam flow are simulated by steam and water injection through the core simulator. The steam production on the primary side of a real, intact-loop

steam generator is simulated by direct steam injection into steam-generator simulators.

Description of UPTF Test 8b Procedures. UPTF Test 8[15] is a separate-effects test to investigate the thermal-hydraulic phenomena that occur in the loops of a PWR as a result of accumulator and low-pressure ECC water injection during the end-of-blowdown, refill, and reflood phases of a postulated LOCA. Pressure and fluid oscillations can occur in the loops induced by direct steam condensation on the injected subcooled ECC water. In a reactor with a cold leg, ECC-water plugs form in the cold leg when the ECC injection rate and the subcooling are high. It should be noted that the formation and movement of these plugs were predicted by TRAC before they were observed experimentally. The goal of Test 8b was to investigate the loop flow pattern and to quantify the thermal-hydraulic boundary conditions that lead to pressure and flow oscillations in the loops when ECC water is injected into the cold legs. The test boundary conditions are given in Fig. 2. The flow parameters that determine water plug formation and oscillation in the loop were of special interest.

The hot- and cold-leg break valves were both open (Loop 4 is the broken loop). The Loop 1 pump simulator was closed. The Loop 2 and 3 pump simulators were set to a stroke of 108 mm (K = 18 at a diameter of 0.750 m) in an attempt to establish a 0.25-bar differential pressure between the upper plenum and downcomer. Loop 4, the broken loop, had a throttle plate with an inner diameter of 0.411 m (K = 18.2 at a diameter of 0.750 m) installed in the hot leg to simulate the flow resistance of a blocked pump. The core simulator steam injection was initiated at 23 s into the test and held constant for approximately 200 s. The cold-leg ECC injection was initiated at 27 s into the test and varied through a series of steps starting at 600 kg/s and decreasing to 80 kg/s. Roughly the first 200 s of Test 8b is a cold-leg-only injection test, with ECC injection occurring in Loop 2 only.

The test conditions for Test 8b were as follows.

Initial pressure in vessel	380 kPa
ECC temperature	311 K
ECC injection rate	80–600 kg/s
Core simulator steam mass flow rate	115 kg/s
Steam-generator steam supply	15 kg/s

Description of the UPTF MOD2 Model. The TRAC-PF1/MOD2 model used in this assessment is the Code Scalability, Applicability, and Uncertainty (CSAU) model.[16] The vessel model for the MOD1 assessment contained 13 axial levels, 3 radial rings, and 4 azimuthal sectors. For the MOD2 assessment, several changes were made in flow areas of cells in the vessel. These were necessary because the MOD2 code requires that the user follow certain noding practices.

A noding diagram for Loop 3, which is typical of an intact loop, is shown in Fig. 3. Loops 1, 2, and 3 are identical. The cold leg of loop 4 (the broken loop) consists of a PIPE and VALVE connected to the VESSEL with a BREAK component

simulating fluid loss to the containment. The pressure at the break is the separator pressure (Fig. 1, unit 3b).

Discussion of UPTF Test 8b Results and Comparisons. At the initial high-ECC injection period of the test, a water plug is formed in the cold leg. The water plug fills the pipe between the injection port and the downcomer. Initially, the plug end toward the downcomer has sufficient breakup and interfacial area such that all of the steam entering from the downcomer is condensed. The oscillation occurs as the plug moves to cover and uncover the injection port. When the injection port is covered, the interfacial area and the condensation rate in the vicinity of the injection port are reduced significantly. The pressure difference between the downcomer and upper plenum is such that with the reduced condensation rate in the cold leg, the plug will start to move toward the downcomer. However, when the injection port is uncovered again, there is a significant increase in the interfacial area condensation near the injection port. This causes low pressure in the vicinity of the injection, which in turn causes the water plug to move back and cover the injection port, starting the oscillation over again. As the ECC injection rates are reduced, the interfacial area and available subcooling become insufficient to condense all of the steam flowing from the downcomer. When this situation occurs, the flow regime in the cold leg switches from a plug flow regime with highly dispersed ends to a stratified flow regime with very little interfacial area. The data indicate that an oscillatory plug flow regime occurs in the cold leg for injection rates from 600 to 250 kg/s. TRAC calculates large-amplitude oscillations ranging from 600 to 400 kg/s. At 250 kg/s, TRAC still calculates an oscillatory flow in the Loop 2 cold leg, but the amplitude is reduced significantly. At 200 kg/s, the pressure and flow data indicate that the oscillatory flow regime has ended. At 200 kg/s, some oscillations continue in the thermocouple response; however, the pressure and flow measurements indicate that the flow in the cold leg is nonoscillatory at 200 kg/s.

The TRAC-calculated upper-plenum pressure and the measured upper-plenum pressure in Fig. 4 indicate that TRAC and the data are oscillatory for 125 s (see Table I). The amplitude of the TRAC pressure oscillation appears to be slightly larger than that observed in the data for the 400- and 600-kg/s ECC injection rates. For the 250-kg/s ECC injection rate, the data indicate a slightly higher amplitude in pressure oscillation. For the 200-, 250-, 400-, and 600-kg/s ECC injection rates, TRAC calculated a higher upper-plenum pressure than observed in the experimental data. However, for the 80- and 150-kg/s ECC injection rates, TRAC calculated a slightly lower upper-plenum pressure. This indicates that TRAC is condensing too much steam at the low ECC injection rates as implied by the upper-plenum pressure.

The Loop 2 cold-leg mass flow rate measurement in the pump loop seal (see Fig. 5) also indicates that TRAC is oscillating with a higher amplitude at the high injection rates than indicated by the data. The flow at this location will be all steam and will come from the upper plenum via the hot leg and come directly from the steam-generator steam injection. For the 400- and 600-kg/s ECC injection rates, TRAC and the data are highly oscillatory with approximately the same frequency; however, the TRAC amplitude appears to be larger. For the 250-kg/s ECC injection rate, the TRAC amplitude is smaller and the frequency is higher than exhibited by

the data. At the 200-kg/s ECC injection rate, both TRAC and the data indicate no significant oscillations.

The Loop 2, Stalk 3, thermocouple data are compared with the TRAC prediction in Fig. 6. Stalk 3 is in the cold leg but close to the downcomer/cold leg connection. The Stalk 3 data support the observations that at high injection rates (600, 400, and 250 kg/s), TRAC is not condensing enough steam. At the low injection rates (200, 150, and 80 kg/s), both TRAC and the data indicate a stratified flow in the cold leg with subcooled water at the bottom and steam at the top. In stratified flow, the cold-leg subcooled fluid temperatures are quite comparable to TRAC values, indicating that the condensation rate in the cold leg is consistent with the UPTF data for stratified flow.

Cold-Leg Modeling Lessons Learned and User Guidelines. Although the model used in TRAC for plug formation and movement is relatively simple, it captures the dominant phenomena. However, we would expect it to be sensitive to noding changes. Therefore, because this is a full-scale experimental facility, it is recommended that all US PWR calculations use noding similar to the noding used to analyze this test. The general guideline used for the noding of the cold legs in the UPTF was to keep the length-to-diameter ratio (L/D) for cells at the injection port and towards the downcomer at ~2.0. The last cell that connects to the downcomer should have an L/D of ~0.8.

Cold Leg Modeling Conclusions. The data from UPTF Test 8b test were compared with the results of calculations performed using TRAC-PF1/MOD2. The results indicate that the code performs satisfactorily when predicting cold-leg plugging and oscillations. The predicted vessel pressure was in good agreement with the data, indicating that the total condensation rate is approximately correct. For high injection rates (400 and 600 kg/s), TRAC predicted the frequency and amplitude of the oscillations in pressure, mass flow rate, and fluid temperature were predicted reasonably well. For low injection rates (200, 150, and 80 kg/s), the transition to stratified flow was predicted accurately. At the ECC injection rate of 250 kg/s, TRAC started the transition to stratified flow earlier than indicated by the data; in addition, the amplitude of the oscillation at 250 kg/s was lower in TRAC than in the data.

TABLE I

ECC INJECTION BOUNDARY CONDITION

Time (s)	Loop 2 ECC Injection Rate (kg/s)
0–29	0.0
33–63	600.0
64–93	400.0
94–123	250.0
124–153	200.0
154–183	150.0
183–213	80.0

UPTF Downcomer Test

UPTF Test 6[17] is a separate-effects test to investigate the steam-water flow phenomenon in the lower plenum and downcomer of a US/Japanese PWR during the end-of-blowdown and refill portions of a cold-leg large-break LOCA. A series of five runs was made under similar boundary conditions to investigate the steam/water CCFL behavior in the full-scale downcomer of a PWR. We will discuss Run 133.

The primary system was filled with dry steam at the start of the test. The primary system pressure corresponds to the containment pressure, and the primary structures were heated to the saturation temperature of the maximum pressure expected during the test. ECC water was injected into the intact-loop cold legs, and nitrogen was injected into the ECC water. Steam was injected into the core simulator and the intact-loop steam-generator simulators.

The test conditions for Run 133 were as follows.

Initial pressure in downcomer	257 kPa
Downcomer wall temperature	460 K
Lower-plenum water inventory	0 kg
Pressure in dry well	256 kPa
ECC temperature	388–390 K
Total ECC-injection rate	1473 kg/s
Total nitrogen-injection rate	1 kg/s
Core simulator steam mass flow rate	110 kg/s
Steam mass flow rate into steam-generator simulators	29–33 kg/s

Because there are three steam-generator simulators capable of steam injection (one in each intact loop), a total of approximately 90 kg/s of steam is injected into the simulators. Because the loops are blocked at the pump simulators, this steam is forced to flow through the hot legs, into the vessel, and up the downcomer. Therefore, the total amount of steam that flows up the downcomer is about 200 kg/s for this test. The steam flow is held fairly constant throughout the test.

The vessel model for the MOD1 assessment contained 13 axial levels, 3 radial rings, and 4 azimuthal sectors. The four loops were simulated using PIPE and TEE components, and the flow conditions were simulated using FILL and BREAK components. The simulation (for the 90-s test) required 197.8 CPU-minutes on a Cray X-MP/48.

One of the most difficult phenomena to predict accurately in a large-break LOCA analysis is the penetration of liquid in the downcomer. It depends on interfacial drag and heat-transfer models, which are in turn dependent on condensation and a reasonable estimate of interfacial surface area. The models used in TRAC are based on a combination of correlations, engineering models, and developmental assessments to produce agreement with available test data. The vessel mass inventory predicted by TRAC and inferred from level data in the UPTF

vessel is compared in Fig. 7. TRAC predicts the trends and total accumulation of water in the vessel quite well.

Reflood Assessment

Description of the CCTF Core-II Facility. The CCTF is an experimental test facility[18] designed to model a full-height core section and four primary loops with components of a PWR. The facility is used to provide information on fluid behavior in the core, downcomer, and upper plenum, including steam and water carryover (steam binding), and integral system (steam generator and pump simulator) effects during the refill and reflood phases of a hypothetical LOCA in a PWR. The central part of the test facility is a nonnuclear core that consists of 1824 electrically heated rods and 224 unheated rods arranged in a cylindrical array. The core is housed in a test vessel that includes a downcomer, lower plenum, and upper plenum as well as a core region. The core design is based on 8 x 8 rod assemblies that model the typical 15 x 15 fuel assemblies of a PWR. Volumetric scaling is based on core flow area scaling.

There were three objectives of the CCTF tests.

1. Demonstration of ECCS behavior during the refill and reflood periods.

2. Verification of reflood analysis codes.

3. Collection of information to improve the thermal-hydraulic models in analysis codes, such as (a) multidimensional core thermal-hydrodynamics, including the radial power distribution effect, fallback effect, and spatial oscillatory behavior; (b) flow behavior in the upper plenum and hot legs; (c) behavior of accumulated water at the bottom of the upper plenum, including possible countercurrent flow and sputtering effects; (d) hydrodynamic behavior of the injected ECC water and the water passing through the steam generator; (e) multidimensional thermal-hydrodynamic behavior in the hot annular downcomer; and (f) overall oscillatory behavior in the system.

The facility was completed on March 10, 1979. Twenty-two tests had been performed with CCTF Core-I by April 1981.[19] The first core was replaced by a new second core in November 1981 for the CCTF Core-II test series. Six tests, including two acceptance tests and two shakedown tests, had been performed with CCTF Core-II by April 1982. The test discussed in this report[18] was a second shakedown test, which is denoted by several names including Test C2-SH2, Test-43, and Run 54. (For the remainder of this paper, we will refer to it as Run 54.) This test was conducted successfully on March 30, 1982. The objectives of the test were to check the functions of the modified CCTF Core-II facility, to confirm the similarities between Core-I and Core-II, and to study the effect of the power supplied into the core. The test was conducted under the same initial and boundary conditions as the base case of the CCTF Core-II test series, except for the supplied power.

The facility was extensively instrumented and included instrumentation to measure the temperatures, absolute pressure, differential pressures, water levels and flow rates. Thermocouples measured the temperatures of the rod surface, fluid, and structure. The absolute pressures are measured in the upper and lower plena, steam generator plena, and containment tanks. The differential pressure measurements are carried out at many locations and cover the system almost completely. A total of 536 data channels was recorded.

After establishing the initial conditions of the Run 54 test, the electric power for preheating was turned off, and the lower plenum was filled to 0.86 m directly from the saturated water tank. When the water level in the lower plenum reached the specified level and other initial conditions of the test stabilized at the allowable tolerance, electric power was applied to the heater rods in the core and the data recording was started. The temperature rises of the rods were monitored by a computer. When a specified initial clad temperature (1003 K) was reached, direct injection (0.104 m^3/s) of the accumulator water into the lower plenum was initiated. The system pressure was maintained at the specified initial pressure (0.2 MPa) throughout the test by controlling the outlet valve of containment tank II. Decay of power input to the rods was programmed to begin when the water reached the bottom of the heated region of the core. The specified initial clad temperature (995 K) of the heater rods for initiation of coolant injection was predetermined by interpolation between the clad temperature (394 K) after preheating and the clad temperature (1073 K) assumed for the time of core bottom recovery. The specified power decay was obtained by normalizing the 1.0 X ANS standard plus ^{238}U capture decay curve at 30 s after shutdown.

When the assumed water level reached the specified level (0.5 m) from the bottom of the heated region of the core, the injection port was changed from the lower plenum to the three intact cold-leg ECC ports. This water level was assumed to be the level at which considerable steam generation occurs in the core to minimize oscillatory behavior resulting from the condensation at the ECC ports. The accumulator injection flow rate then was reduced to 0.088 m^3/s in the cold-leg injection period. At a specified time (16.5 s) after the time of core bottom recovery, the valves in the accumulator lines and low-pressure coolant injection (LPCI) circulation lines were closed and the valves in LPCI injection line were opened. These actions transferred the ECC injection from accumulator injection mode to LPCI mode. A specified LPCI flow rate (0.0116 m^3/s) was maintained constantly until the ECC injection was turned off.

The generated steam and the entrained water flowed to the containment tanks via broken and intact loops. The steam then was vented to the atmosphere to maintain a constant pressure in the containment tanks. After all thermocouples on the surface of the heater rods indicated quenching of the rods, the power supply to the heater rods was decreased linearly. The linear power decay was performed to study any particular reflood phenomena under very low power supply. The linear power decay was initiated at 690.5 s, and the power was turned off at 898 s. After the ECC injection was turned off, the recording system was stopped, thus terminating the test.

TRAC Calculation Results. We performed two calculations with different nodalizations for the reactor vessel. The base calculation was essentially a straightforward conversion of an earlier TRAC-PF1 deck that was used for the analysis of CCTF Run 54 done as part of the 2D/3D program.[20,21] The base calculation used what is referred to as the "intermediate-node model" of the CCTF reactor vessel. The vessel noding includes 2 azimuthal zones, 4 radial rings, and 16 axial levels. An alternative vessel nodalization was used that consisted of 1 azimuthal zone, 4 radial rings, and 22 axial levels. The additional axial detail was added in the core region.

In addition to renodalizing the reactor vessel from a 2-theta, 16-level model to a 1-theta, 22 level model, 21 heat slabs were added in the 1-theta model to specifically model heat conduction across the core barrel. The maximum number of fine-mesh heat conductors also was raised from 100 to 250, and the criteria for inserting fine-mesh heat conductors were changed to cause more fine-mesh conductors to be used.

Figure 8 shows a comparison between the 1-theta model results, the 2-theta model results, the original TRAC-PF1 calculation, and the experimental results for the hot rod at the core midplane. This figure shows calculated and measured temperatures at the location of the highest measured temperature during the test. The TRAC-PF1/MOD2 code with the 2-theta model is in closer agreement with the experimental results than the original TRAC-PF1 calculations at near the time when the peak temperature is reached, although the time of the peak and the quench time are predicted more closely by the original TRAC-PF1 calculation. The resulting comparisons between the 1-theta model, the 2-theta model, and the original TRAC-PF1 calculation are summarized in Table II.

TABLE II

COMPARISON OF CALCULATION RESULTS FOR CALCULATED MIDPLANE TEMPERATURE

	Peak Temperature (K)	Time of Peak (s)
CCTF Experimental Data (TE30Y17)	1092	125
Original TRAC-PF1 Calculation	1029	111
TRAC-PF1/MOD2 (2-Theta Model)	1080	153
TRAC-PF1/MOD2 (1-Theta Model)	1105	144

The cladding temperatures and the quench times are generally well predicted by all of the TRAC code versions at the lower elevations. At the core midplane and up to the higher elevations, the peak cladding temperatures are generally well predicted, but the heat transfer later in the transient appears to be under-predicted by the TRAC-PF1/MOD2 code versions. As a consequence, the cladding temperatures decrease too slowly, and the quench is predicted too late. At the highest elevations,

the cladding temperatures are under-predicted. The TRAC-PF1/MOD2 calculated cladding temperatures tend to be more oscillatory than the experimental results or the original TRAC-PF1 calculation. The cause of this behavior currently is not understood.

The calculated differential pressures in the lower plenum, core lower half, and core upper half are in generally good agreement with the experimental results in the lower plenum and the lower half of the core. The code under-predicts the differential pressure in the upper half of the core. This is consistent with the under-prediction of the rod heat transfer at the higher elevations. In general, the loop parameters are in relatively good agreement with the experimental results

Reflood Conclusions. The maximum cladding temperatures are calculated more accurately with the MOD2 code than with the MOD1 code, and the running time is shorter. The heat transfer appears to be under-predicted in the upper elevations as a result of the under-prediction of the liquid inventory at the upper elevations of the core. The CCTF Run 54 calculations are not very sensitive to axial or theta nodalization differences.

LOFT Large-Break LOCA Test L2-6

Description of LOFT Facility. The LOFT facility is a 50-MWt PWR with instrumentation to measure and provide data on the thermal-hydraulic condition throughout the system. The facility is configured to represent a 1/60-scale model of a typical 1000-MWe (electric) commercial four-loop PWR. Three PWR primary-coolant loops are simulated by a single intact loop in LOFT scaled to have the same volume-to-power ratio. A broken loop in LOFT simulates the fourth PWR primary-coolant loop, where a break may be postulated to occur. The facility consists of a reactor vessel with a nuclear-fueled core; an intact loop with an active steam generator, pressurizer, two primary-coolant pumps (PCPs) connected in parallel, and an ECC injection system that includes two low-pressure injection-system (LPIS) pumps, two high-pressure injection-system (HPIS) pumps, and two accumulators; and a broken loop with a simulated PCP, a simulated steam generator, two quick-opening blowdown valves, a blowdown suppression tank, and low-flow warmup lines that are connected to the intact loop. The intact-loop active steam generator has a secondary side consisting of a U-tube boiler section, steam dome, and downcomer. The steam-generator secondary side is connected to a main steam-flow control valve (MSFCV), condenser, feedwater pump, auxiliary-feedwater pump, and a feedwater-flow control valve. References 22 and 23 contain additional details of the LOFT test facility.

Description of the LOFT Test Procedure. Experiment L2-6 simulated a 200% cold-leg break. The nozzles installed in the broken-loop cold and hot legs have an inside diameter of 0.1032 m. The broken hot-leg nozzle is downstream from the passive steam generator and pump simulators. The break is initiated by opening quick-opening blowdown valves downstream from the nozzles; these valves open in ~20 ms.

The ECC system injects into the intact cold leg and provides a scaled amount of ECC to represent the injection into three loops. The primary-coolant pumps trip at 0.8 s and coast down under the influence of the flywheels. When the pump speed

drops below 73.54 rad/s, the flywheel uncouples from the pump and effectively reduces the pump moment of inertia. The assumption of loss of off-site power at the initiation of the transient results in a delay in the availability of the HPIS and LPIS. The experiment operating specifications[24] and the quick-look report[25] document the test initial conditions and operation.

The behavior of this test is quite similar to that of earlier Tests L2-2 and L2-3 in which the pumps run at approximately constant speed throughout the test. The most significant differences occur in the core during the first ~11 s. Because of the higher power level in Test L2-6, the peak cladding temperatures are higher (that is, 1074 K vs ~900 K previously). This test exhibits the early core rewet observed in L2-2 and L2-3; however, in the completed Test L2-6, rapid quenches are observed from cladding temperatures as high as 1074 K. Also, the early rewet only progresses to a core elevation between 1.113 and 1.245 m before a second temperature increase begins, whereas L2-2 and L2-3 exhibit complete quenching of the entire core during the early rewet.

Description of the TRAC-PF1/MOD2 Model. The noding diagrams of the TRAC representation of the LOFT facility are given in Ref. 2. The noding scheme and input are based on the TRAC-PD2 model, which was modified for TRAC-PF1/MOD1 by Los Alamos, improved and modified by UKAEA, and then modified again for TRAC-PF1/MOD2 by Los Alamos.

Steady-State and Transient Calculations. Constrained steady-state (CSS) input was added to the UKAEA LOFT input deck for the MOD2 code. These CSS controllers drive the steady-state solution to the user-desired loop flow rate, secondary-side pressure, and cold-leg temperature. The resulting MOD2 initial conditions are given in Table III.

The MOD2-calculated pressure is compared with the measured pressure for the intact-loop hot leg in Fig. 9. The pressure comparison is excellent through the subcooled blowdown and the initial phase of the two-phase blowdown. During the two-phase blowdown, TRAC depressurized slightly faster than indicated by the data. However, the difference is not significant. The pressure predicted by TRAC is slightly higher than indicated by the data during the reflood phase of the transient.

Figure 10 is a data comparison of the broken-loop hot-leg mass-flow rate between TRAC and the measured quantity. The TRAC predictions are within the error bands included with the mass-flow-rate data. The spike during the subcooled blowdown is well-predicted by TRAC. The surge of two-phase liquid during the two-phase blowdown is also well-predicted by TRAC. A similar data comparison for the broken cold leg is given in Fig. 11. For the broken cold leg, the subcooled blowdown spike in mass flow and two-phase blowdown mass flow rates are predicted very accurately by TRAC. During the reflood, TRAC calculates significant slugs of the emergency cooling system (ECS) fluid that move down the broken cold leg. Similar behavior is observed in the experimental data, as indicated in Fig. 11.

The measured accumulator level is compared with the TRAC prediction in Fig. 12. The comparison indicates that TRAC accurately calculates the time required to empty the accumulator and therefore accurately calculates the ECS flow rate into the intact cold leg.

The initial fuel rod stored energy is well-predicted by the MOD2 code as indicated in Figs. 13 and 14. Both the fuel centerline and fuel surface temperature measurements indicated adequate comparisons during the first 10–20 s of the LOFT transient. Figures 13 and 14 also indicate that the TRAC quench is delayed approximately 10 s, as compared with the experimental data. Fuel rod centerline temperature (Fig. 13) data indicate approximately the correct integrated transient cooling and an approximately 10-s delay in quenching in TRAC as compared with the data.

TABLE III

LOFT TEST L2-6 INITIAL CONDITIONS

Parameter	Measured Value		TRAC-PF1/MOD2
Reactor power (MW)	46.0	±1.2	47.0
Intact-loop mass flow (kg/s)	248.7	±2.6	248.0
Hot-leg pressure (MPa)	15.09	±0.08	15.03
Hot-leg temperature (K)	589.0	±1.1	591.0
Cold-leg temperature (K)	555.9	±1.1	556.7
Pressurizer steam volume (m^3)	0.39	±0.02	0.31
Pressurizer liquid volume (m^3)	0.607	±0.02	0.64
Steam-generator pressure (MPa)	5.62	±0.10	5.62
ECC A-system accumulator			
Pressure (MPa)	4.11	±0.06	4.11
Temperature (K)	302.0	±6	322.0

The fuel rod surface temperature (Fig. 14) data and TRAC-calculated results are quite comparable early in the transient (during the first 5 s). Both the data and the TRAC results indicate a cooling of the fuel surface as the reactor power decreases and the blowdown transient starts and then a heat-up of the fuel surface as the cladding begins to heat up rapidly. When the blowdown quench begins, both the data and TRAC results indicate a decrease. The large difference between the TRAC results and the data as the transient proceeds may be a result of the fuel pellet surface temperature thermocouple reading being closer to the cladding temperature than the actual fuel surface temperature. For example, between 30 and 40 s, the data indicate a fuel surface temperature of 520–600 K, whereas the fuel centerline temperature during this same time period is 750–800 K. TRAC indicates that the decay heat power levels are insufficient to support such a large temperature gradient across the fuel during this time period. Therefore, it is assumed that the fuel surface temperature measurement is influenced by the cladding temperature during this time. However, the fuel surface measurement does indicate that rod quenching in TRAC is delayed by 10–15 s as compared with the data.

Figures 15 and 16 indicate that TRAC is doing an excellent job of predicting the peak cladding temperature and doing an adequate job of predicting the blowdown quench or cooling transient. We believe that with the external thermocouple (T/C) model developed by UKAEA, we would have additional cooling during the blowdown. However, the external T/C model is incompatible with the implicit axial conduction model developed by JAERI, and we currently cannot use both models at the same time. Time to quench is predicted within 10 s of the experimental data. These results are a significant improvement over previous TRAC-PF1/MOD1 and TRAC-PD2/MOD1 published results.

LOFT L2-6 Conclusions. The MOD2 code reflood and quench models accurately model the dominant phenomena in LOFT L2-6. The MOD2 hydrodynamic models for blowdown, refill, and reflood are accurate.

LARGE-BREAK LOCA ANALYSIS

The CSAU MOD1 input deck was converted to MOD2 input to investigate the code speed-up of the 3D two-step numerics in the MOD2 code as compared with those in the MOD1 code. The peak clad temperatures for the nominal large-break LOCA calculation for the CSAU input deck are given in Figs. 17–19. Version 14.3 tends to calculate a lower blowdown PCT because the Version 14.3 steady-state calculation had too high a cold-leg temperature. The high cold-leg temperature resulted in early flashing of the cold-leg fluid, which resulted in an early core blowdown quench. The Version 14.4 and MOD2 steady-state calculations obtained an accurate initial cold-leg temperature, which resulted in a later core blowdown quench and a slightly higher blowdown PCT.

With the improved downcomer models in Version 14.4 and in the MOD2 code, the core reflood starts ~5 s earlier than in the Version 14.3 calculation. Both the Version 14.4 and the MOD2 code calculations tend to reflood the core faster than the Version 14.3 code calculation. The MOD2 core essentially is quenched by 50 s into the transient.

The CPU times for these three calculations are shown in Fig. 20. The MOD2 code runs much faster than either of the MOD1 codes. The major difference in run times between these calculations is the 3D two-step in the MOD2 code allows time-step size to increase significantly over the Courant number. The CSAU model included a several small hydro cells in the VESSEL component, which were used to simulate leakage flow paths between the downcomer and upper plenum regions in the vessel component. These small hydro cells tended to hold the MOD1 time-step sizes back, whereas they had no major effect on the MOD2 time-step sizes. The MOD2 time-step sizes tended to be controlled by how rapid the transient progressed.

REFERENCES

1. Safety Code Development Group, "TRAC-PF1/MOD1: An Advanced Best Estimate Computer Program for Pressurized Water Reactor Thermal-Hydraulic Analysis," Los Alamos National Laboratory report LA-10157-MS, NUREG/CR-3858 (July 1986).

2. J. W. Spore et al., "TRAC-PF1/MOD2 Developmental Assessment Manual," Los Alamos National Laboratory report in preparation.

3. K. O. Pasamehmetoglu et al., "TRAC-PF1/MOD2 Theory Manual," Los Alamos National Laboratory report in preparation.

4. J. H. Mahaffy, "A Stability Enhancing Two-Step Method for Fluid Flow Calculations," J. Comp. Phys. **46**, 329-341 (1982).

5. "Upper Plenum Test Facility (UPTF) Test No. 8 Cold/Hot Leg Flow Pattern Test U9 316/88/11," Siemens AG, Energy Technology, Mechanical and Process Engineering Laboratories, Erlanger Quick Look Report (September 1988).

6. Y. Murao et al., "Data Report on Large Scale Reflood Test-43—CCTF Core-II Shakedown Test C2-SH2 (RUN 054)," Japan Atomic Energy Research Institute memo 58-155 (1983).

7. D. L. Batt et al., "Experimental Data Report for LOFT Anticipated Transient Experiments L6-1, L6-2, and L6-3," Idaho National Engineering Laboratory/EG&G report EGG-2067, NUREG/CR-1797 (December 1988).

8. S. G. Bankoff et al., "Countercurrent Flow of Air/Water and Steam/Water through a Horizontal Perforated Plate," Int. J. Heat Mass Transfer **24**(3), 1381-1395 (1981).

9. G. DeJarlais and M. Ishii, "Inverted Annular Flow Experimental Study," Argonne National Laboratory report ANL-85-31, NUREG/CR-4277 (1985).

10. D. D. Taylor et al.,"TRAC-BD1/MOD1: An Advanced Best Estimate Computer Program for Boiling Water Reactor Transient Analysis," EG&G report EGG-2294, NUREC/CR-3633 (April 1984).

11. L. A. Crotzer, "TRAC-PF1/MOD2 TEE Component Offtake Model: A Completion Report," Los Alamos National Laboratory report LA-UR-91-4052 (November 1991).

12. H. Akimoto, Y. Abe, and Y. Murao, "Implementation of an Implicit Method into Heat Conduction Calculation of TRAC-PF1/MOD2 Code," Japan Atomic Energy Research Institute memo 01-008 (February 1989).

13. "American National Standard for Decay Heat Power in Light Water Reactors," American Nuclear Society Standard ANSI/ANS-5.1 (1979).

14. K. O. Pasamehmetoglu et al.,"TRAC-PF1/MOD2 Theory Manual," Los Alamos National Laboratory report in preparation.

15. "Upper Plenum Test Facility (UPTF) Test No. 8 Cold/Hot Leg Flow Pattern Test U9 316/88/11," Siemens AG, Energy Technology, Mechanical and Process Engineering Laboratories, Erlanger Quick Look Report (September 1988).

16. B. Boyack et al., "Quantifying Reactor Safety Margins: Application of Code Scaling, Applicability, and Uncertainty Evaluation Methodology to a Large-Break, Loss-of-Coolant Accident," EG&G report EGG-2552, NUREG/CR-5249 (October 1989).

17. "2D/3D Program Upper Plenum Test Facility, Test No. 6, Downcomer Countercurrent Flow Test U9 316/89/2," Siemens AG Quick-Look Report (March 1989), Sec. IV.II.2.

18. Y. Murao et al., "Data Report on Large Scale Reflood Test-43—CCTF Core-II Shakedown Test C2-SH2 (Run 054)," Japan Atomic Energy Research Institute memo 58-155 (1983).

19. Y. Murao et al., "Analysis Report on CCTF Core-I Reflood Tests," Japan Atomic Energy Research Institute memo 57-057 (1982).

20. C. J. Crowley and P. H. Kothe, "TRAC-PF1 Calculation of CCTF Core II Reflood Test 54 (C2-SH2)," Los Alamos National Laboratory 2D/3D Program Technical Note LA-2D/3D-TN-86-2 (March 1986).

21. C. J. Crowley, M. W. Cappiello, and B. E. Boyack, "Summary Report of TRAC-PF1 Assessment Against the CCTF-Core II Data," Los Alamos National Laboratory document in preparation.

22. D. L. Batt and J. M. Carpenter, "Experiment Data Report for LOFT Anticipated Transient Experiments L6-1, L6-2, and L6-3," Idaho National Engineering Laboratory/EG&G report EGG-2067, NUREG/CR-1797 (December 1980).

23. C. L. Nalezny, "Summary of Nuclear Regulatory Commission's LOFT Program Experiments," Idaho National Engineering Laboratory/EG&G report EGG-2248, NUREG/CR-3214 (July 1983).

24. H. B. Robinson, "LOFT System and Test Description (Loss-of-Coolant Experiments Using a Core Simulator)," Idaho National Engineering Laboratory report TREE-NUREG-1019 (November 1976).

25. C. D. Keeler, "Best-Estimate Prediction for LOFT Nuclear Experiments L6-1, L6-2, L6-3, and L6-5," Idaho National Engineering Laboratory/EG&G report EGG-LOFT-5161 (October 1980).

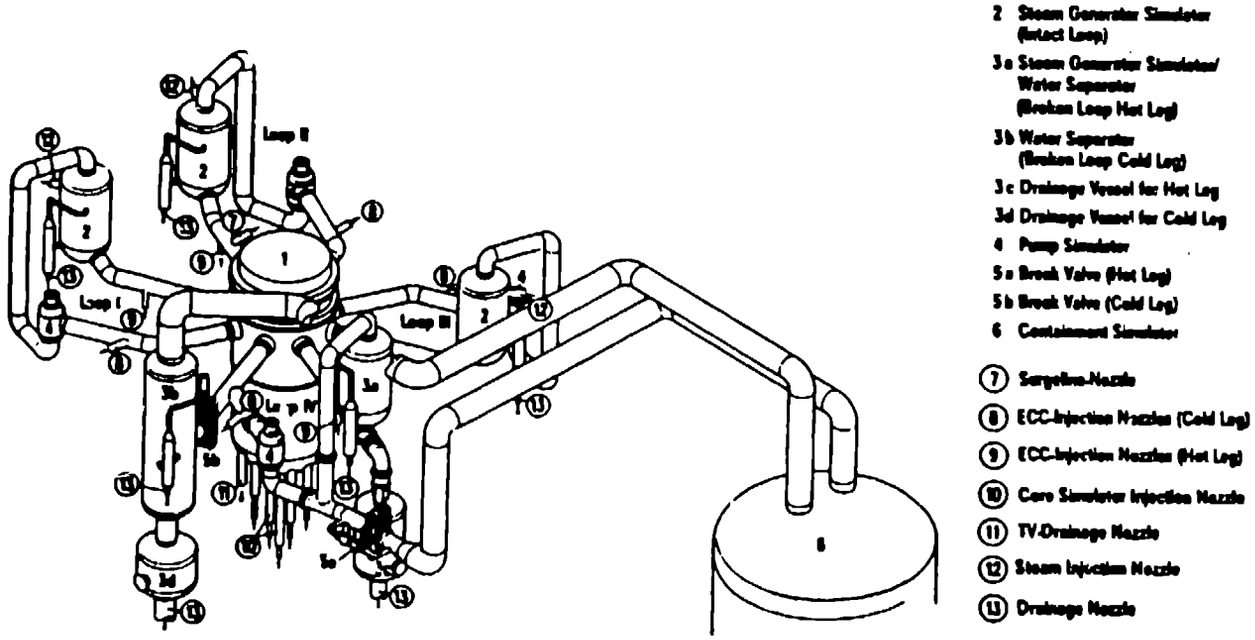

Fig. 1.
UPTF primary system.

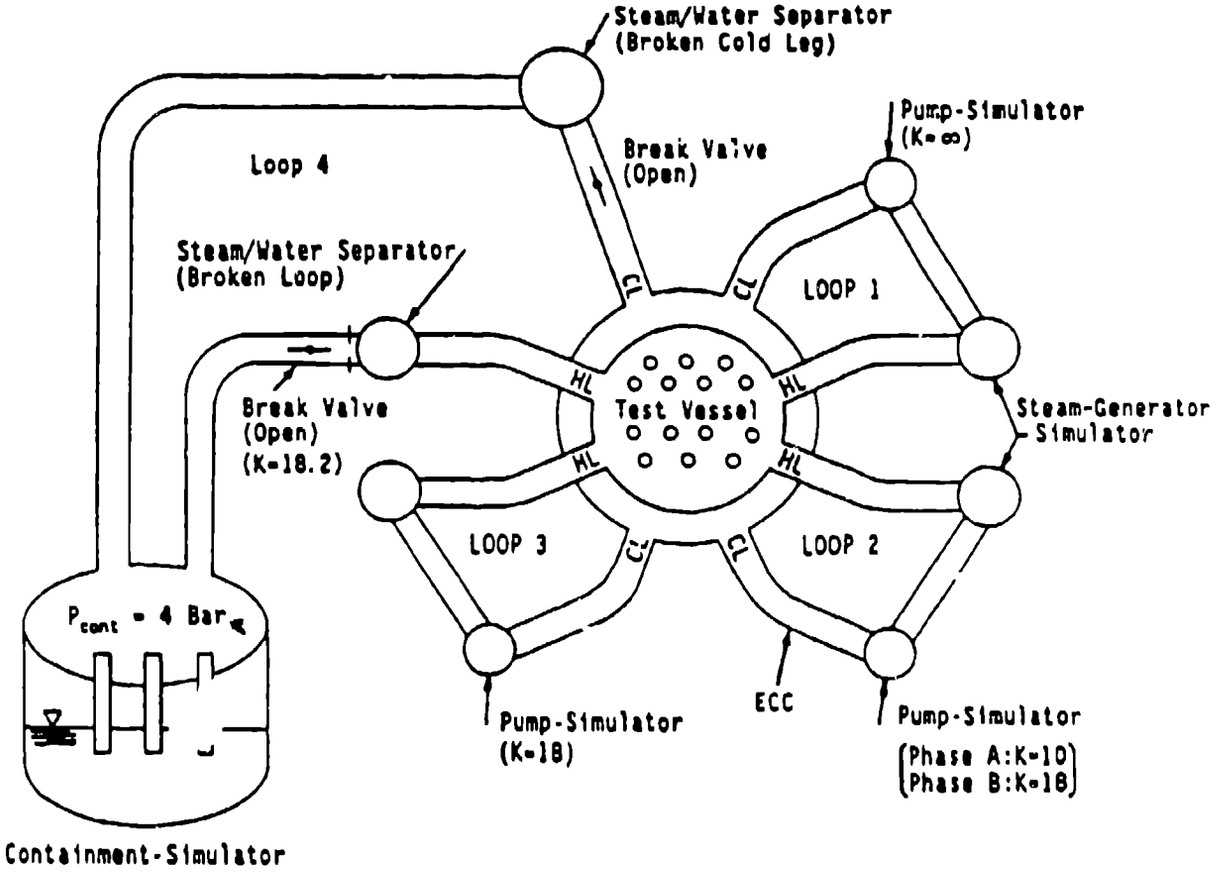

Fig. 2.
Test boundary conditions for Test 8b.

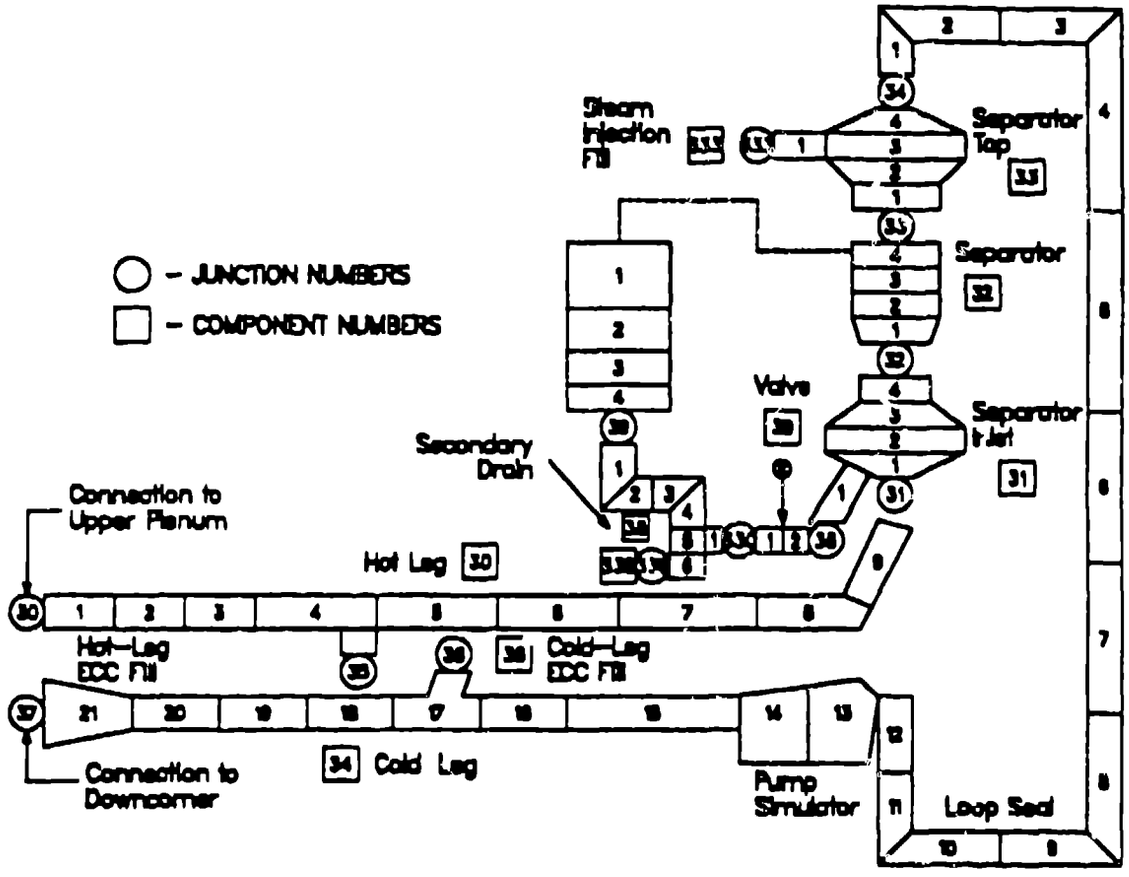

Fig. 3.
Noding diagram for Loop 3.

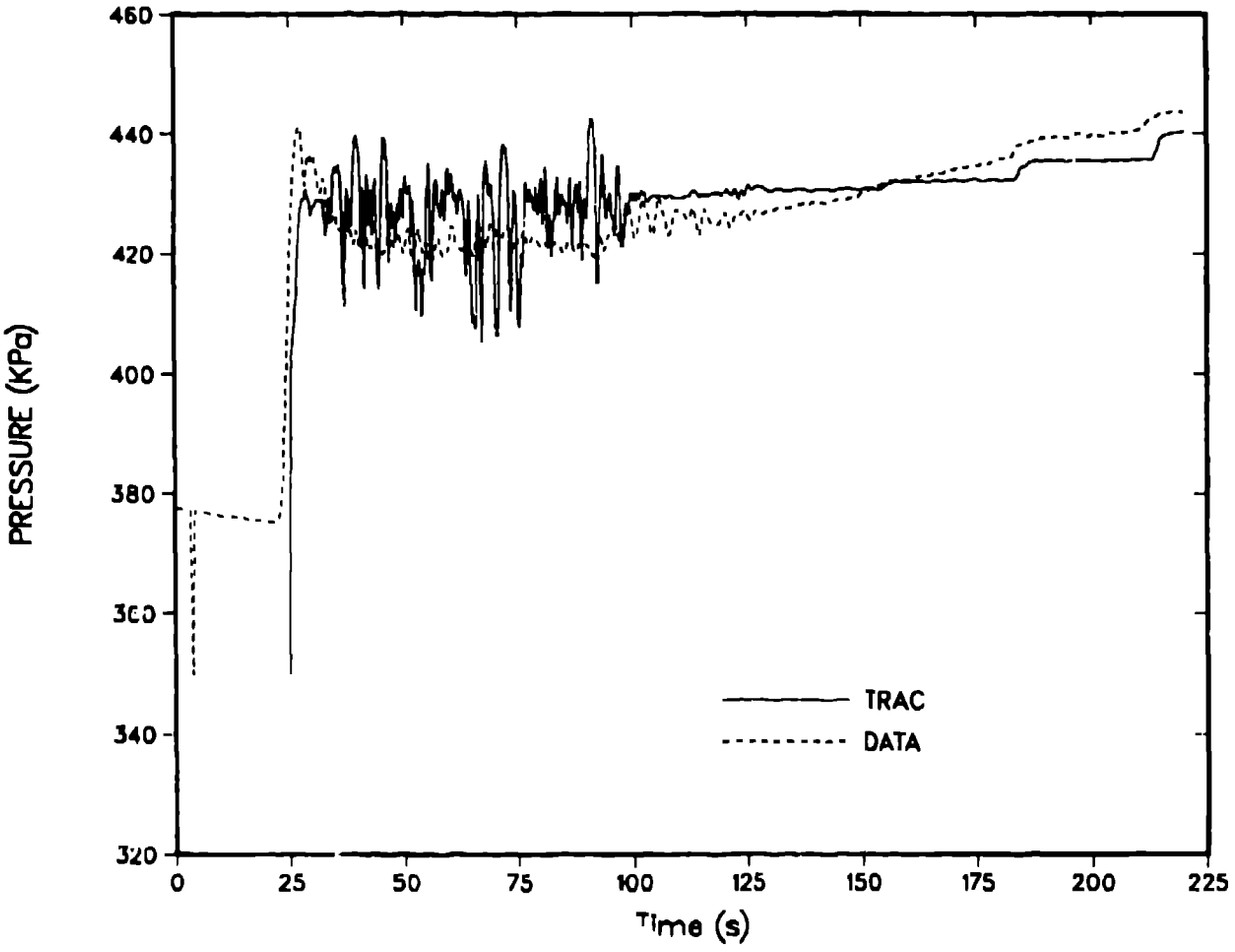

Fig. 4.
Upper-plenum pressure and TRAC data comparison.

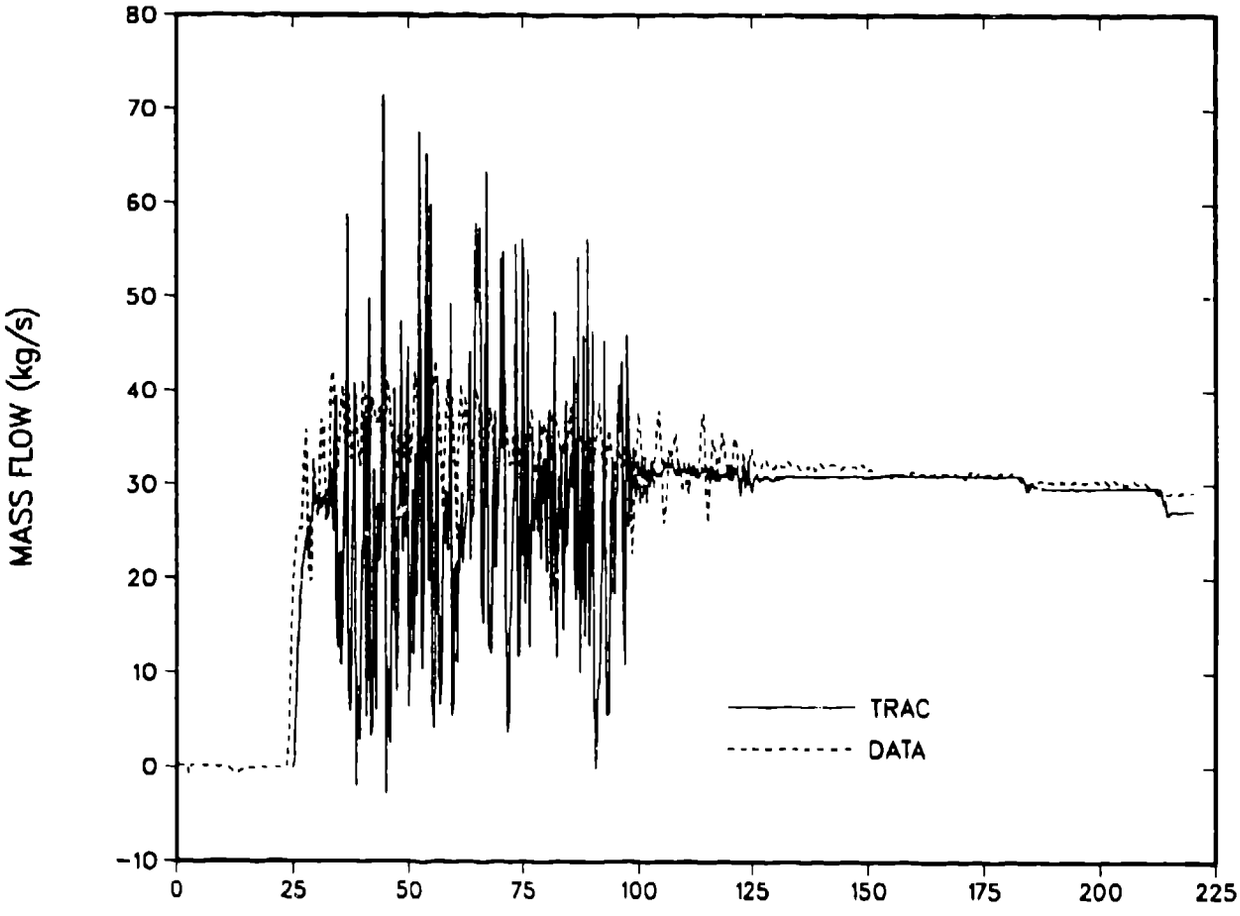

Fig. 5.
Cold-leg mass flow and TRAC data comparison.

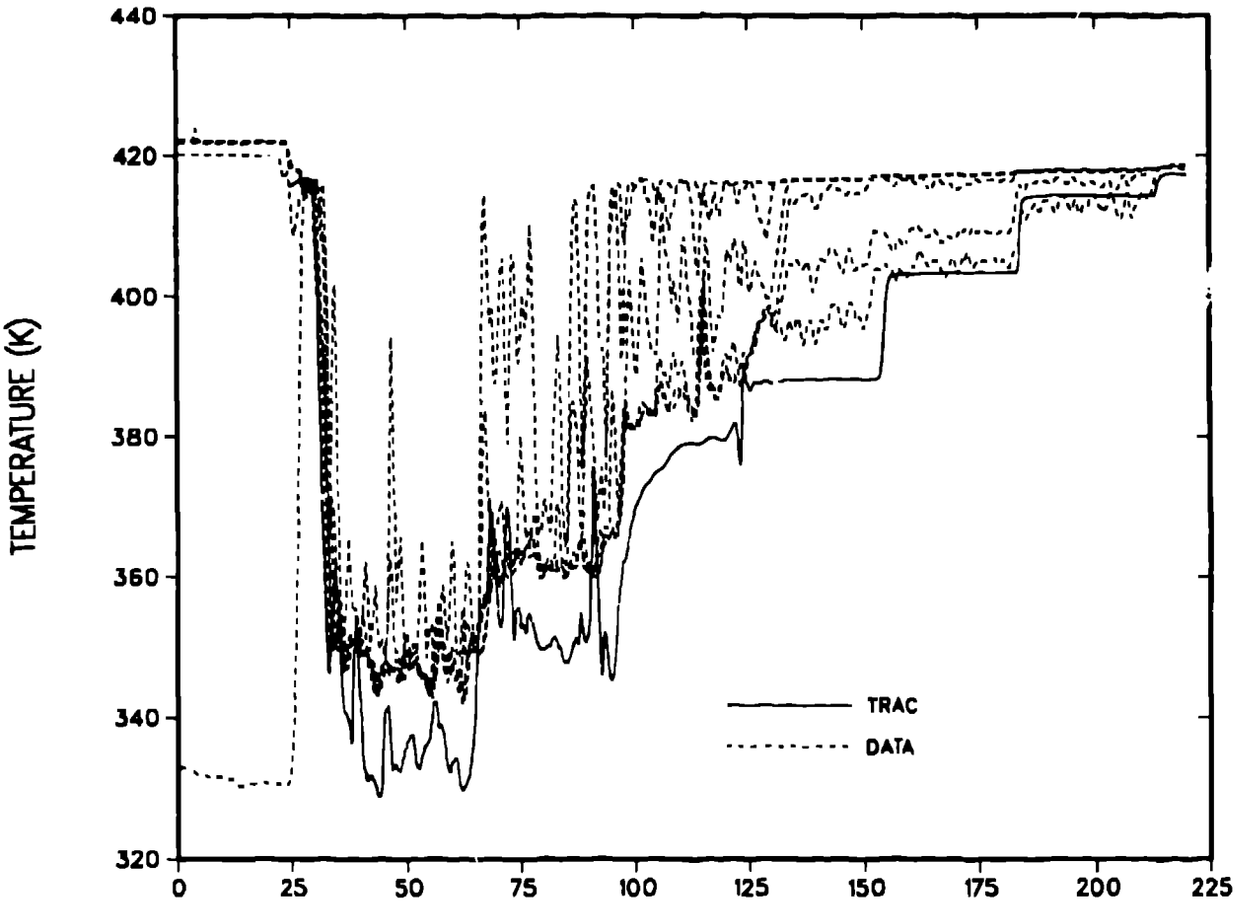

Fig. 6.
Stalk 3 thermocouple and TRAC data comparisons.

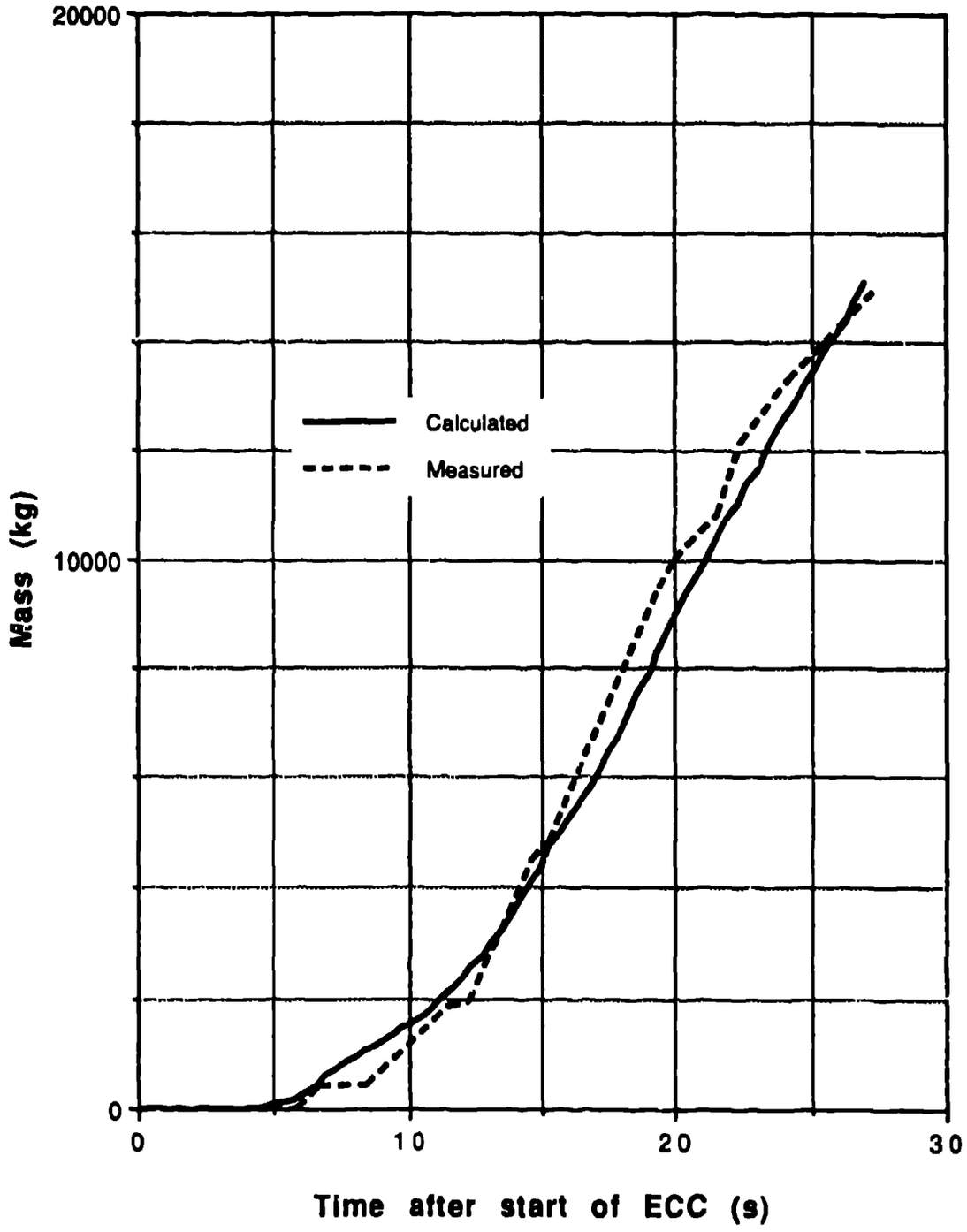

Fig. 7.
Comparison of calculated and measured mass inventory in vessel.

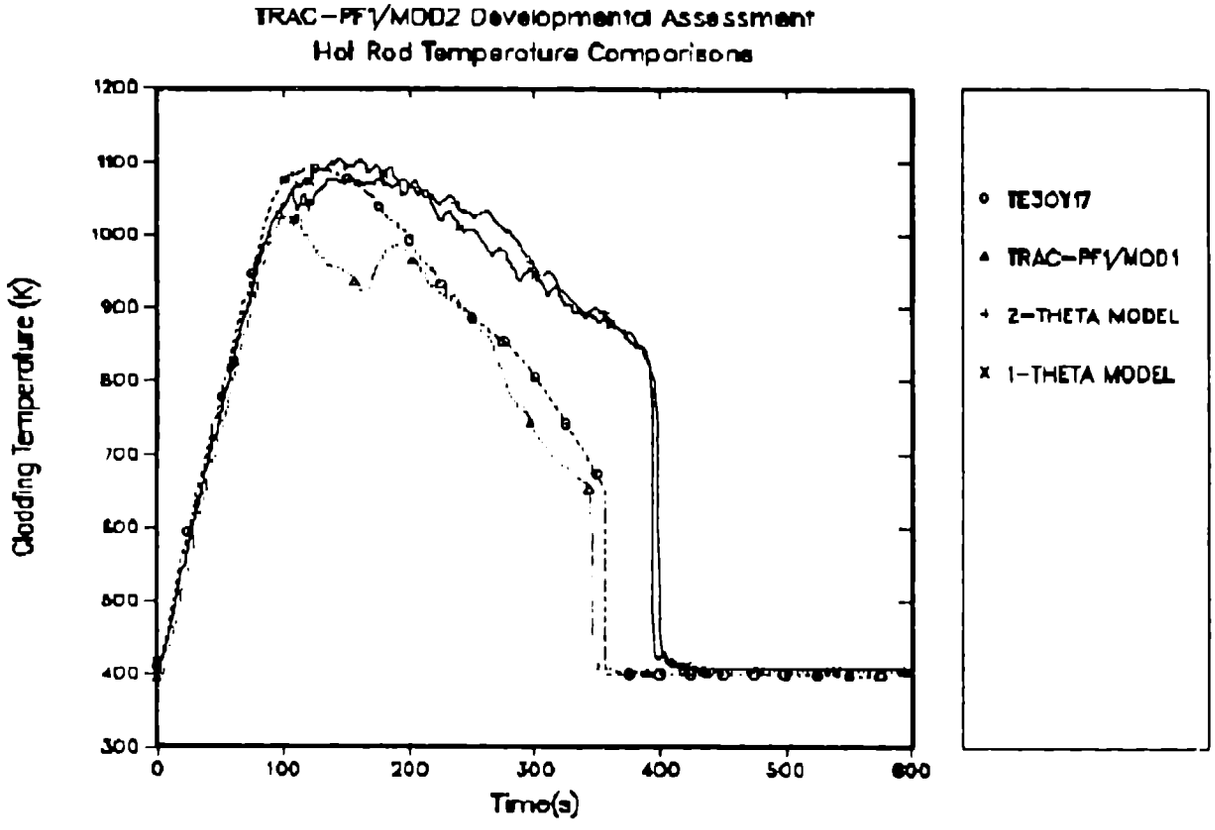

Fig. 8.
Comparison of 1- and 2-Theta Model calculated and measured cladding temperatures for the hot rod at the core midplane.

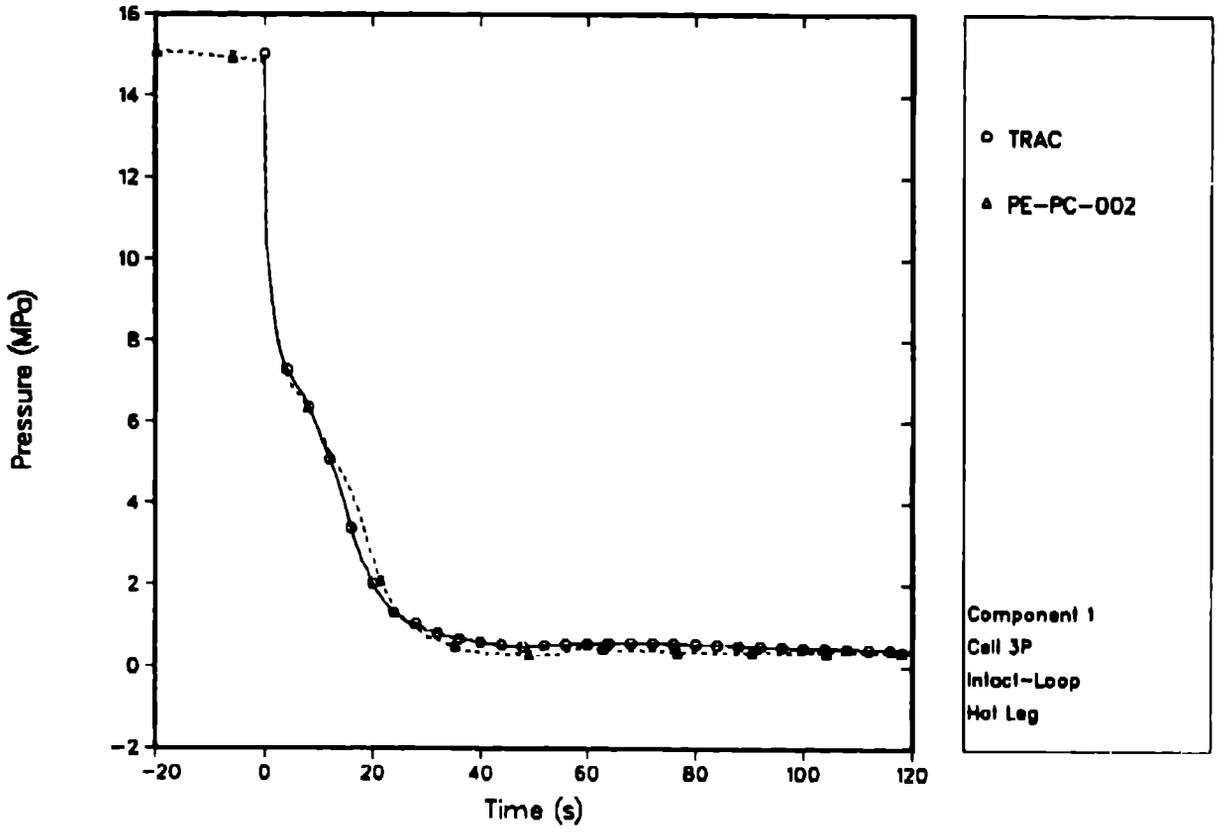

Fig. 9.
Intact-loop hot-leg pressure.

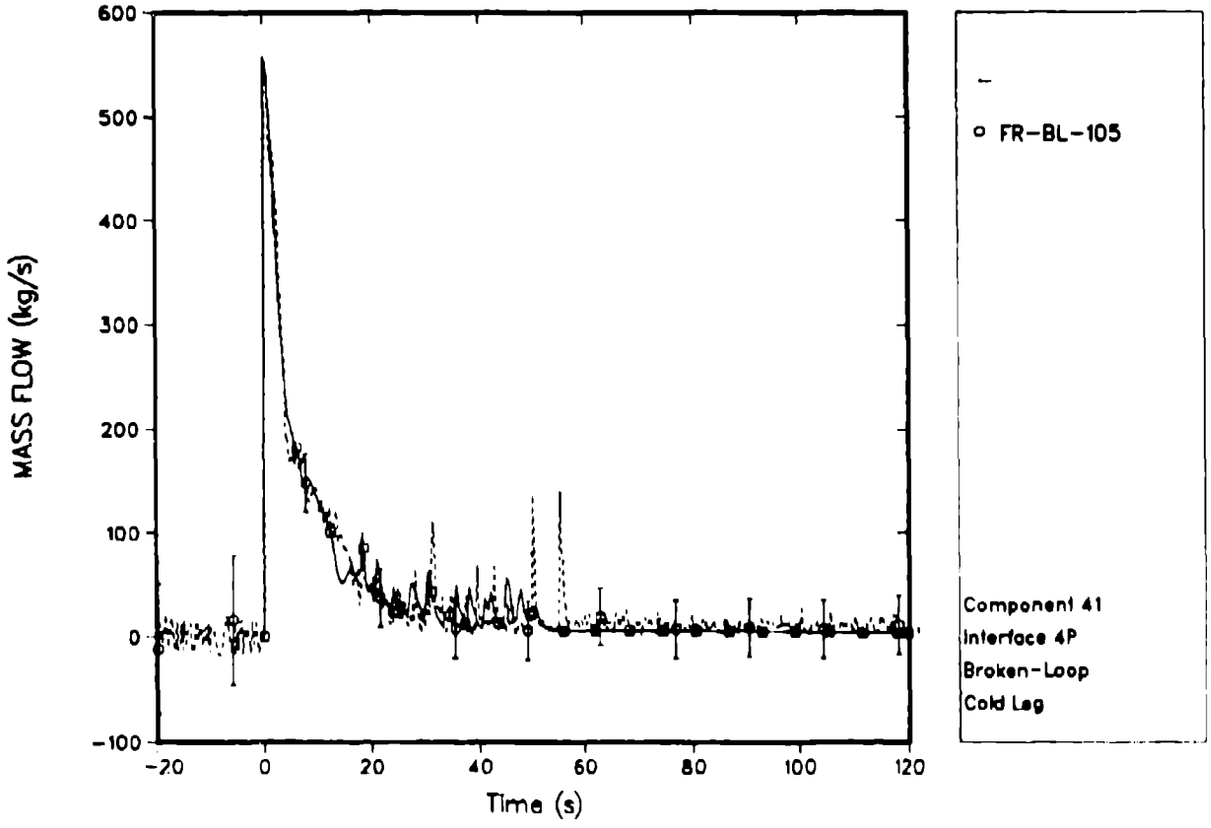

Fig. 10.
Broken-loop hot-leg mass flow.

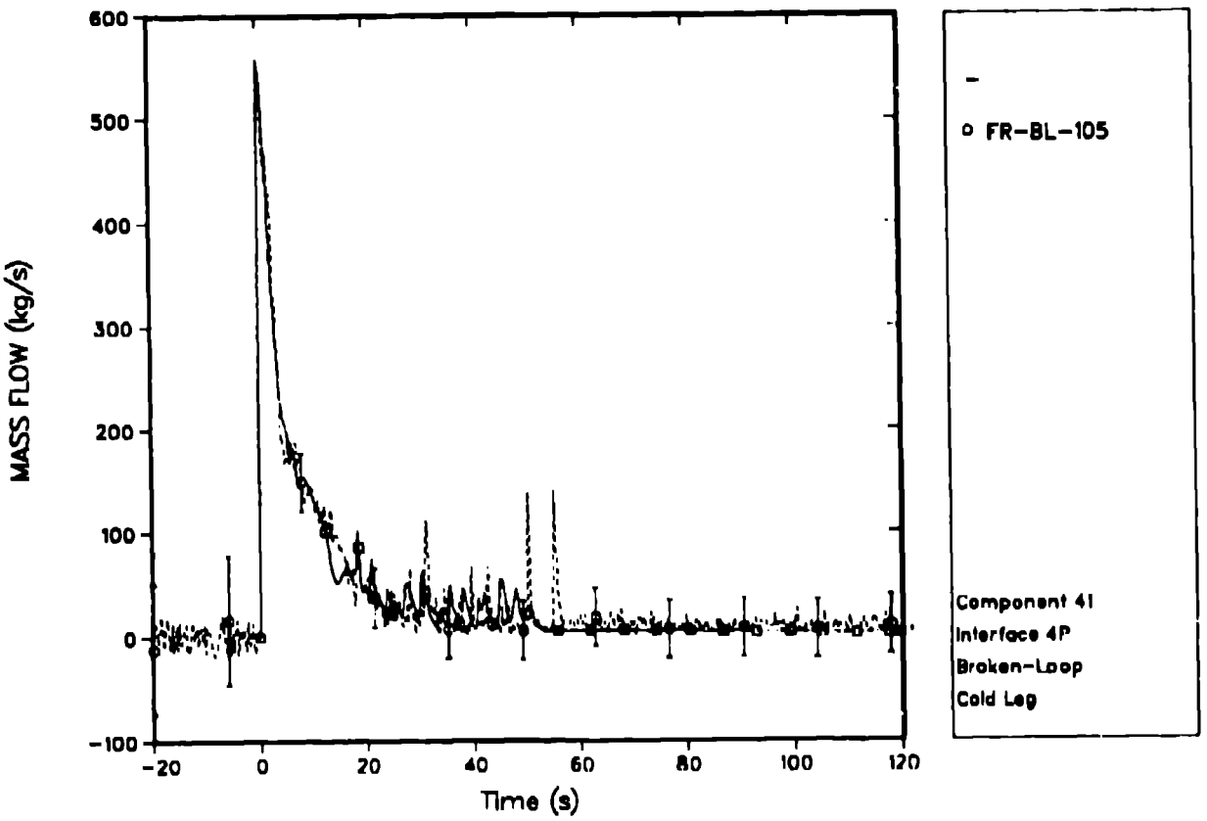

Fig. 11.
Broken-loop cold-leg mass flow.

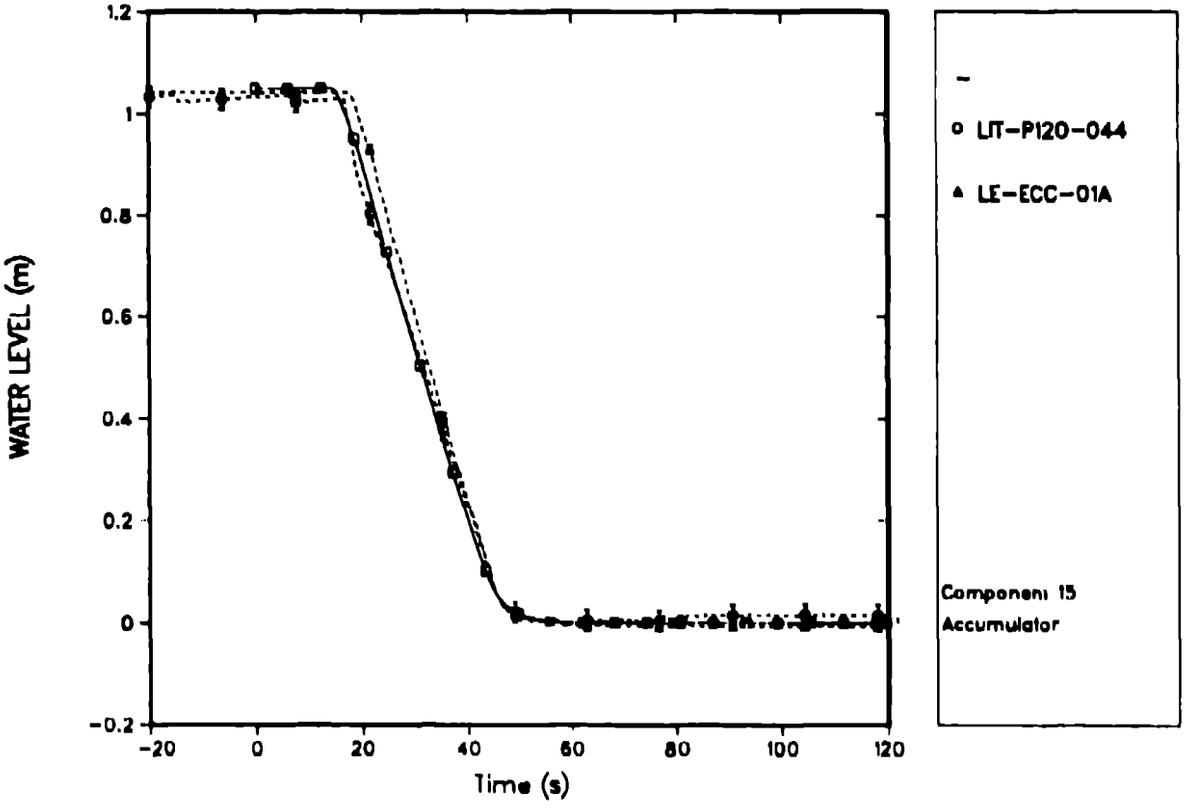

Fig. 12.
Accumulator level comparison.

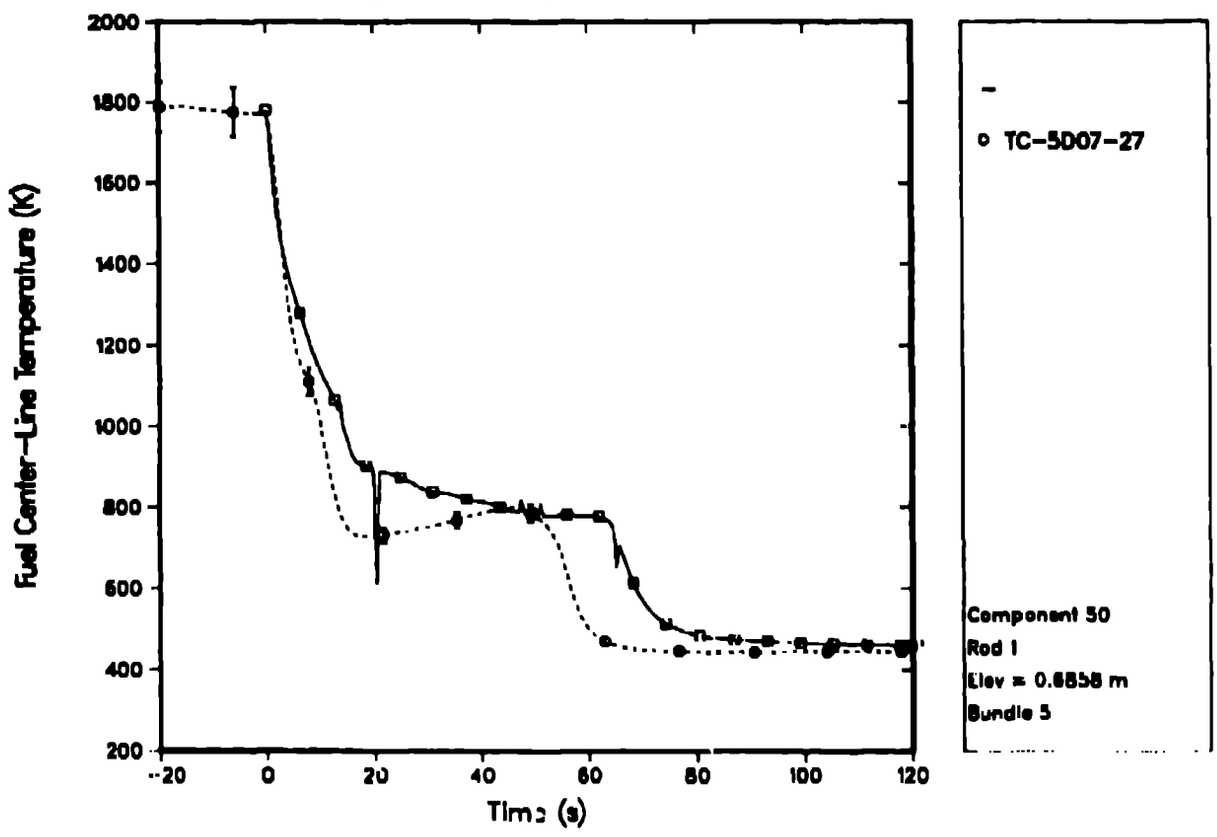

Fig. 13.
Centerline fuel, temperature; Rod 1 elevation = 0.6858 m.

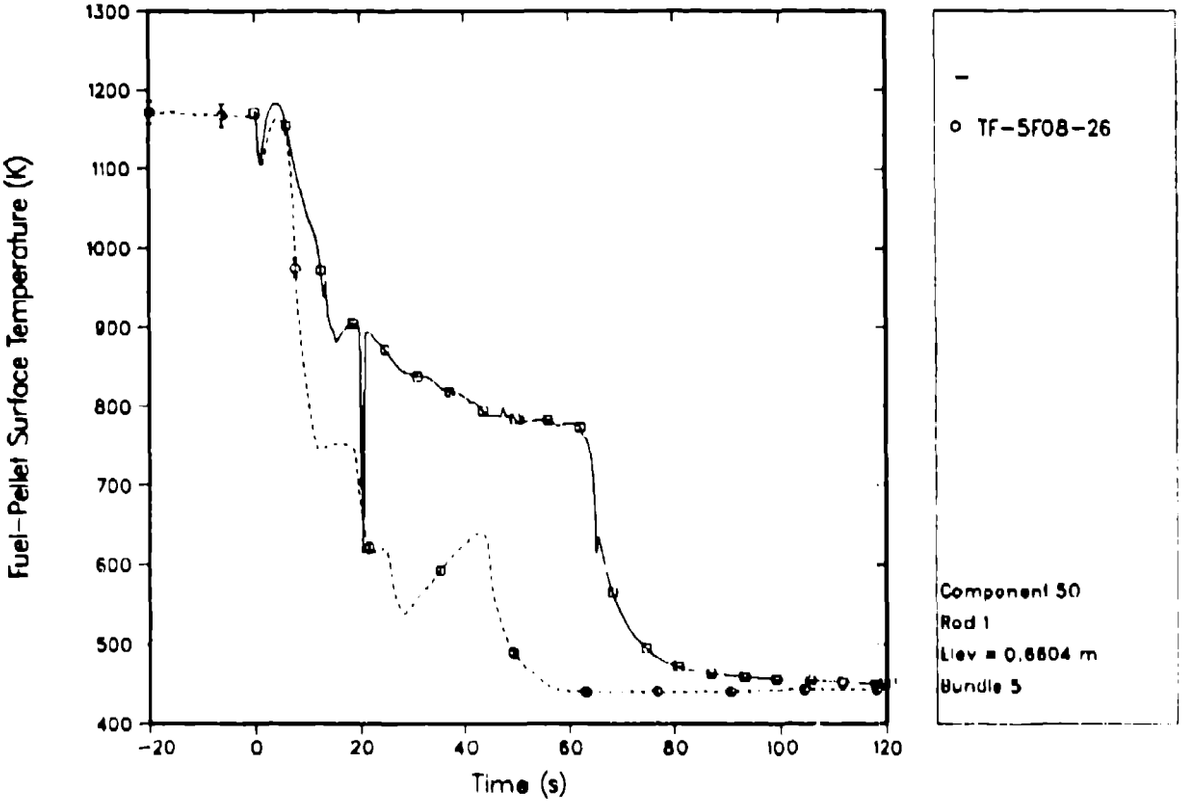

Fig. 14.
Pellet surface temperature; Rod 1 elevation = 0.6604 m.

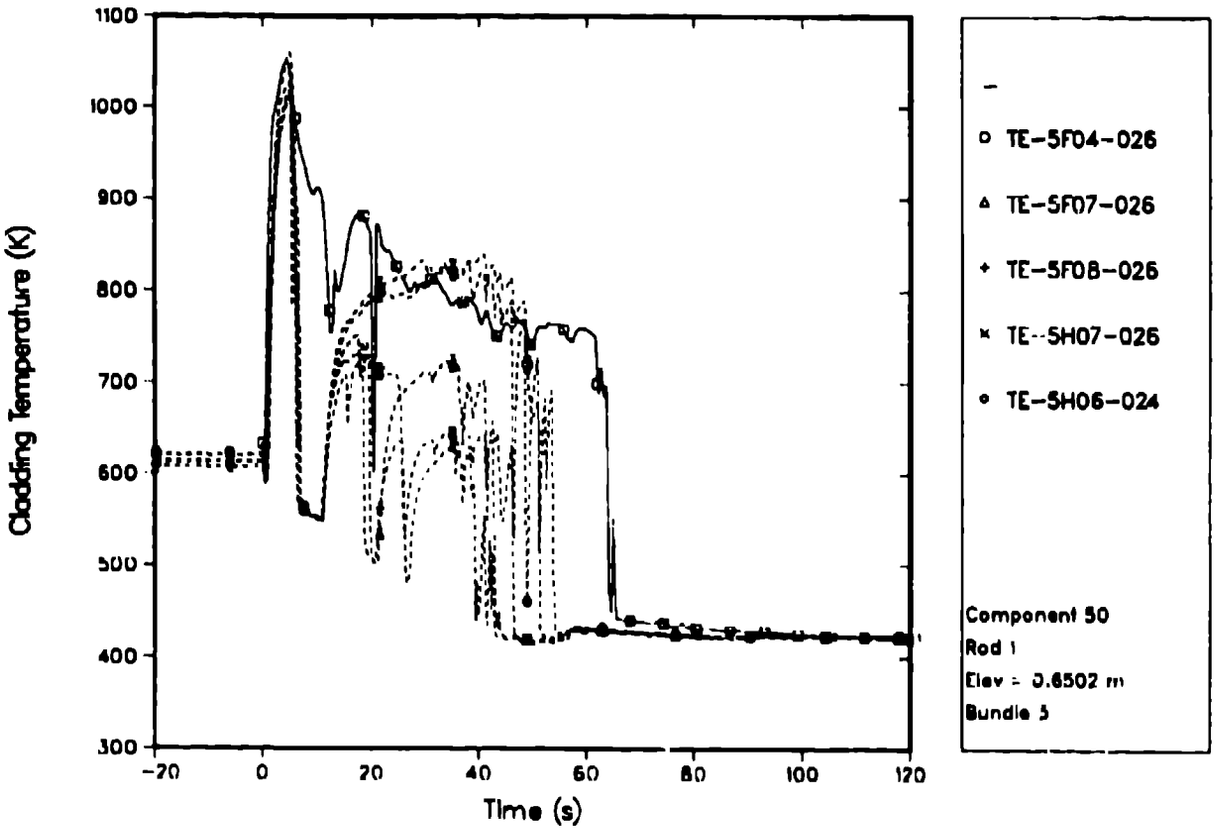

Fig. 15.
Cladding temperature; Rod 1 elevation = 0.6502 m.

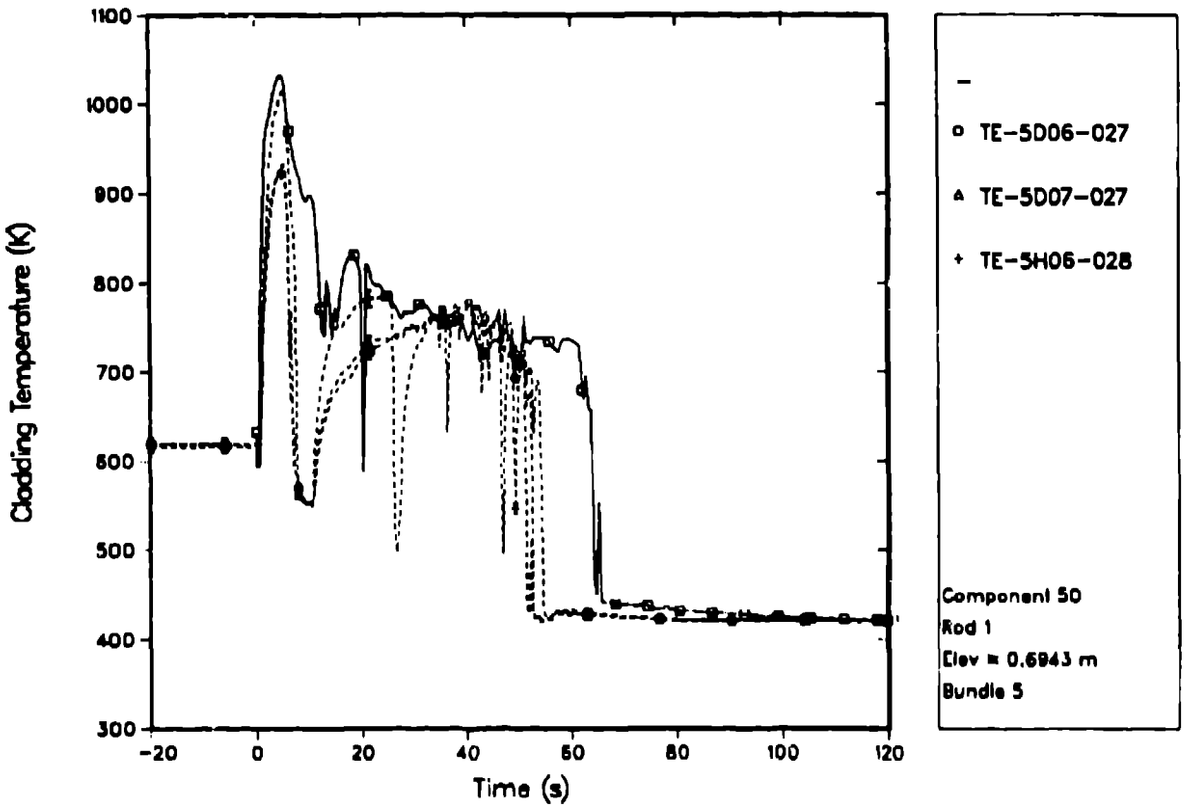

Fig. 16.
Cladding temperature; Rod 1 elevation = 0.6943 m.

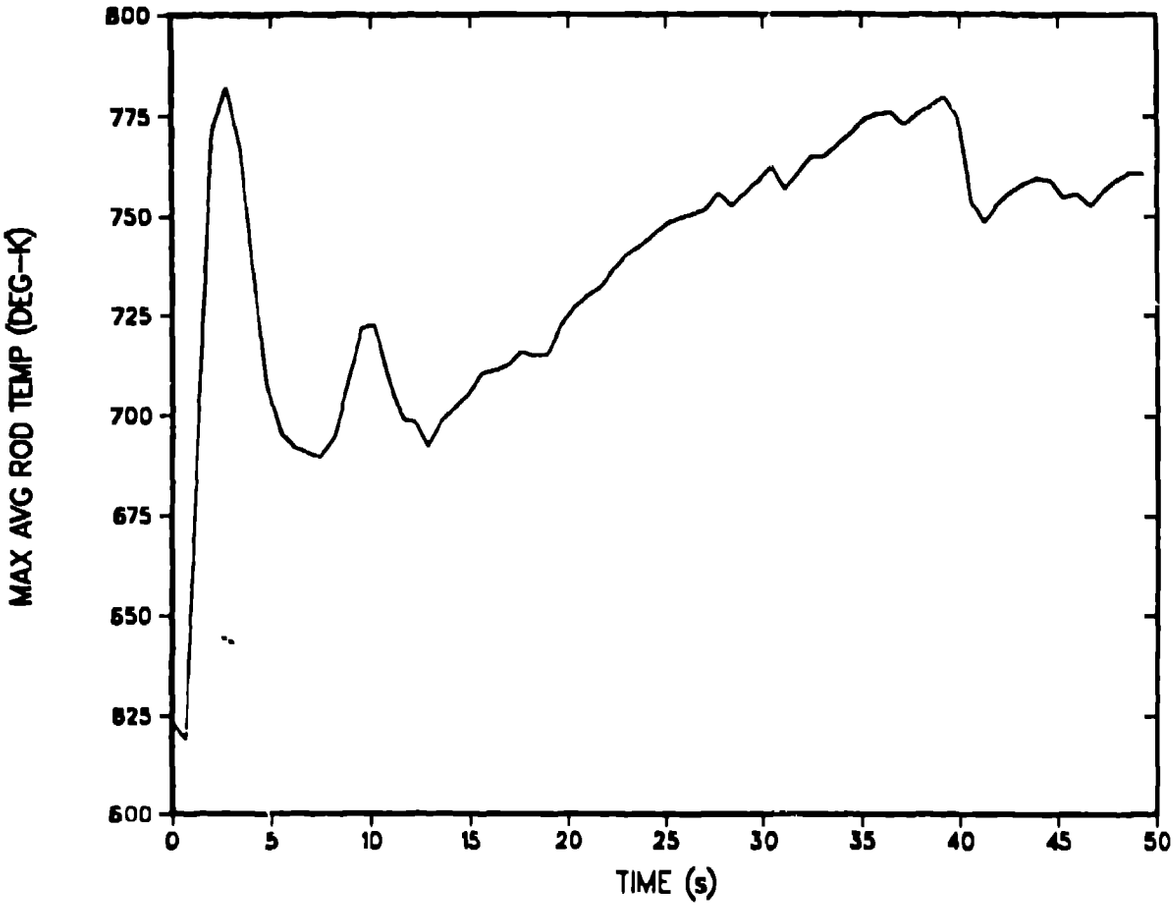

Fig. 17.
Peak cladding temperature for Version 14.3.

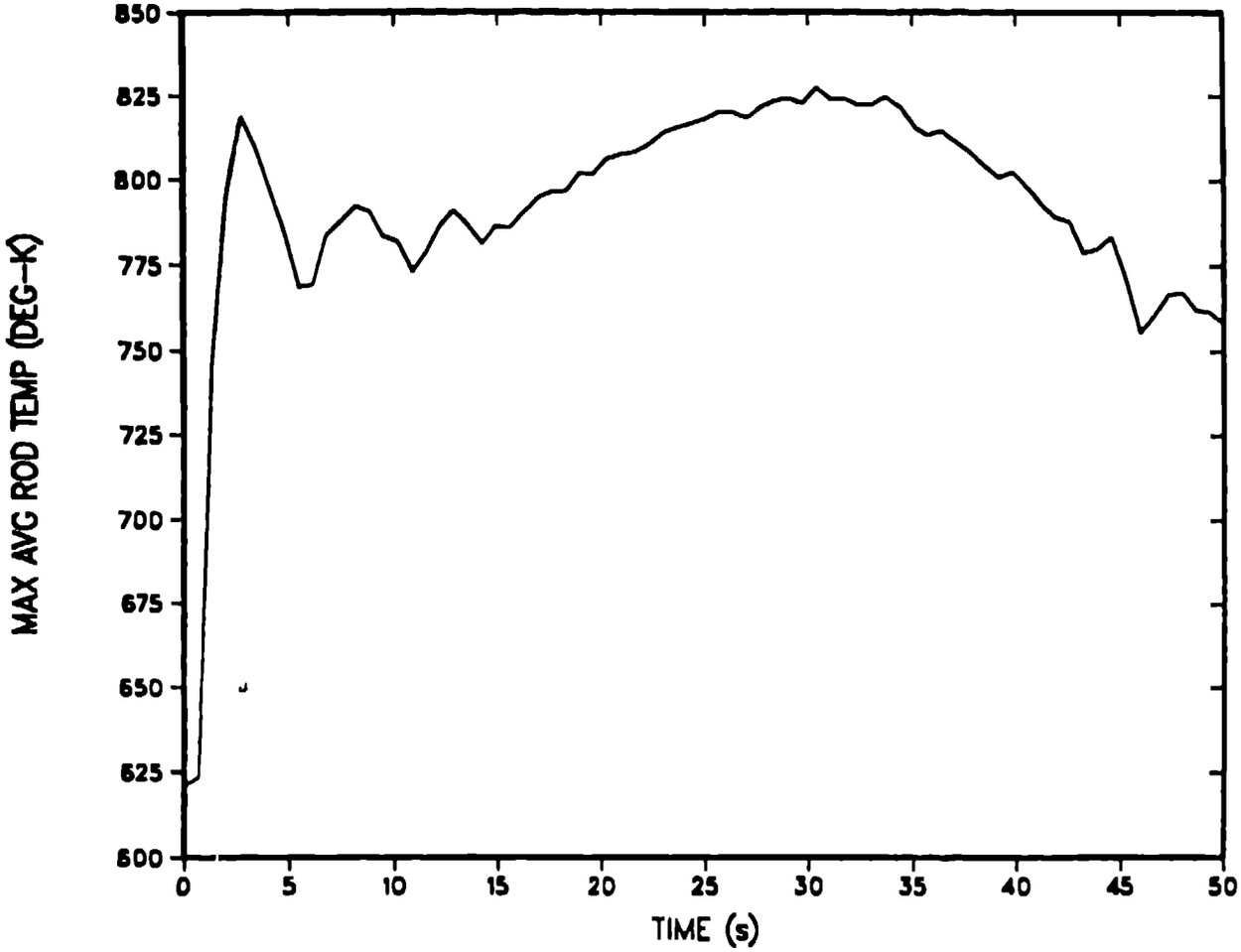

Fig. 18.
Peak cladding temperature Version 14.4.

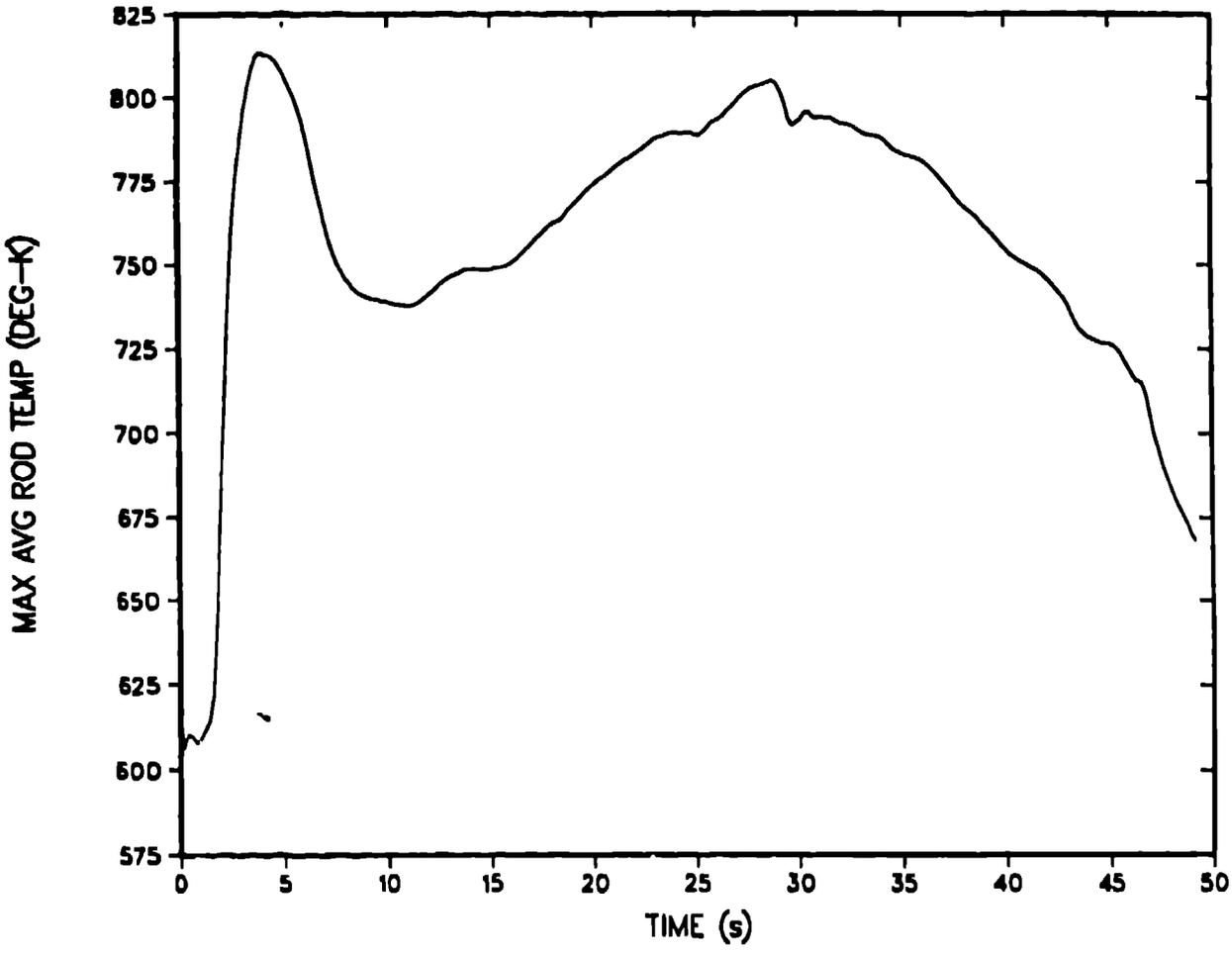

Fig. 19.
Mod2 peak cladding temperature.

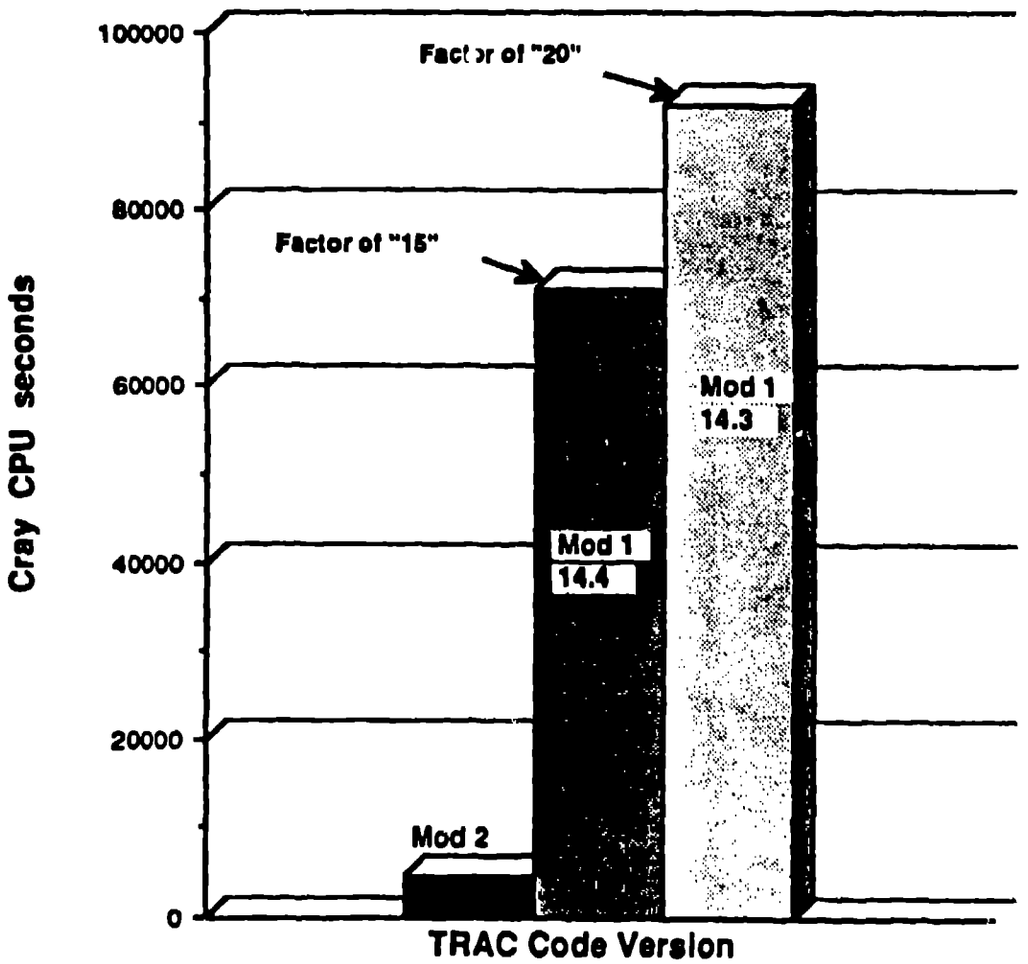

Fig. 20.
Computer run time comparison.
- WPWR LBLOCA, CSAU Input Deck
- 50 s of transient time